Why Do Vanadium Atoms Form Multiple-Decker Sandwich Clusters with Benzene Molecules Efficiently?

Tomokazu Yasuike, Atsushi Nakajima, Satoshi Yabushita, and Koji Kaya*

Department of Chemistry, Faculty of Science and Technology, Keio University, 3-14-1 Hiyoshi, Kohoku-ku, Yokohama 223, Japan

Received: January 16, 1997; In Final Form: April 22, 1997[⊗]

Transition-metal benzene clusters, $M_n(benzene)_m$ (M = Ti, V, and Cr), were synthesized by the reaction of laser-vaporized metal atoms with benzene vapor. All the clusters exhibit magic number behavior at $m = n + 1$, which is rationalized by the structure of a multiple-decker sandwich, but V atoms can efficiently take the sandwich structure (up to $n = 5$) in particular. This metal specificity of the V atoms and their growth mechanism were examined by quantum chemical calculations, the full valence configurational interaction (FVCI) method with configuration-averaged SCF orbitals. The calculation results imply that (1) total spin conservation in growth process plays an important role and (2) the production in the sandwich clusters particularly favors a process through lower spin states. The combination between experimental and theoretical investigations leads us to a better comprehension of both the bonding scheme in the sandwich clusters and the growth mechanism, and accordingly, a more efficient production method is proposed generally for the transition-metal sandwich complexes.

1. Introduction

The development of the laser vaporization method has enabled us to synthesize various kinds of transition metal clusters in the gas phase. Several groups independently have succeeded in the synthesis of metal−molecule complexes in the gas phase by modifying the laser vaporization method.[1−7]

Recently, we have reported the preparation of the multiple-decker sandwich clusters, $V_n(C_6H_6)_{n+1}$ ($n = 1-5$).[8] From the organometallic point of view, the formation of such clusters is very interesting. Since the discovery of ferrocene,[9] many sandwich complexes have been investigated. For example, by the combination of the first-row transition metal atoms and C_5H_5 or C_6H_6, various sandwich complexes such as $M(C_6H_6)_2$ (M = Ti, V, and Cr) and $M(C_5H_5)_2$ (M = Ti, V, Cr, Mn, Fe, Co, and Ni) have been synthesized.[10] Although organometallic chemists have tried to synthesize not only double-decker sandwich complexes such as $M(C_6H_6)_2$ and $M(C_5H_5)_2$ but also multiple-decker sandwich complexes, this attempt has been realized only partly. To our knowledge, synthesized multiple-decker complexes containing unsubstituted C_5H_5 or C_6H_6 as the ligand molecule were only the $Ni_2(C_5H_5)_3$ cation[11] and $(C_5H_5)V(C_6H_6)V(C_5H_5)$.[12] For triple-decker sandwich complexes, Lauher et al. have proposed the 30/34 valence electron rule.[13] However, the numbers of valence electrons are 30, 26, and 28 for the $Ni_2(C_5H_5)_3$ cation, $(C_5H_5)V(C_6H_6)V(C_5H_5)$, and $V_2(C_6H_6)_3$, respectively. Therefore, it is not clear whether their valence electron rule is valid or not.

To probe experimentally the reason vanadium atoms form multiple-decker sandwich clusters with benzene molecules, we changed the metal atom from vanadium to titanium or chromium. Although the differences among these three atoms are small with respect to their numbers of valence electrons, the experimental results showed significant metal specificity in the formation of multiple-decker sandwich clusters.

The metal specificity of their reactivity in the gas-phase reaction has been investigated extensively because of their importance as the reaction center of the catalyst. Kaldor and co-workers have studied the reaction between transition-metal clusters and organic molecules and pointed out that the reactivity of clusters correlates with their ionization energies.[14] Especially, the adsorption reaction of the hydrogen molecule requires electron donation from the cluster to the hydrogen antibonding σ_u orbital, and its correlation is clear. The chemistry of transition-metal cations has been developed by Armentrout and co-workers.[15] By control of the translational energy for reaction, much information has been obtained on the reactivity of the metal cations. Their key concepts for understanding the metal-specific reactivity are the conservation of spin multiplicity during the reaction and the importance of the electronic configuration of metal atom cations. These concepts are very useful and well established. Although the reaction of neutral atoms is very interesting, products having no charge make it difficult to detect reaction products and to interpret experimental results. Nevertheless, Hackett and co-workers[16] and Weisshaar and co-workers[17] have traced the decay of reactants and have found that the $3d^n4s^2$ electronic configuration of the first-row transition metals is not favorable for reacting with molecules. Hackett and co-workers have also reported that neutral Cr[18] and Fe[19] atoms are nonreactive toward benzene in the gas phase.

These consequences of previous experimental work are very useful for interpreting our experimental results but not enough. Therefore, we also calculated the potential energy curves for $M-C_6H_6$ systems (M = Ti, V, and Cr). For $M_n(C_6H_6)_m$ systems, there are only few theoretical studies with the post-HF methods including electronic correlation. Recently, Bauschlicher et al. have performed the MCPF calculations for the $M(C_6H_6)^+$ (M = Sc, Ti, V, Cr, Mn, Fe, Co, Ni, and Cu).[20] King et al. have calculated the dissociation energies (metal−arene) for $M(C_6H_6)_2$ (M = Ti, Zr, Hf, Cr, Mo, and W) at the MP2 level.[21] As for the potential energy curves, there is only the work by Roszak and Balasubramanian for the $Pt^+-C_6H_6$ system with the CASSCF method.[22]

2. Methodology

2.1. Experiment. Details of the experimental setup have been provided elsewhere.[8] Briefly, $M_n(C_6H_6)_m$ (M = Ti, V,

[⊗] Abstract published in *Advance ACS Abstracts,* June 15, 1997.

S1089-5639(97)00243-0 CCC: $14.00

and Cr) clusters were synthesized by the reaction between laser-vaporized atoms and benzene molecules. First, metal atoms were vaporized by the irradiation of the second harmonic of a pulsed Nd^{3+}:YAG laser (532 nm) and vaporized hot metal atoms were cooled to room temperature by a pulsed He carrier gas (10 atm). Second, the cooled atoms were sent into a flow-tube reactor where benzene vapor seeded in a He gas was injected in synchronization with the flowing of the atoms. The M_n-$(C_6H_6)_m$ clusters thus generated were sent into the ionization chamber through a skimmer and were intersected with the light of an ionization laser, an ArF excimer laser (6.42 eV), or second harmonic of a dye laser by an XeCl excimer laser. The photoions were mass-analyzed by a time-of-flight (TOF) mass spectrometer with reflectron.

In the *adiabatic* ionization energy (E_i) measurement, the photon energy of the second harmonic of the dye laser was changed at ~0.015 eV intervals in the range 5.9−3.5 eV, while the abundance of the $M_n(C_6H_6)_m$ clusters was monitored by the ionization of the ArF laser. The fluences of both the tunable ultraviolet (UV) laser and the ArF laser were monitored by a pyroelectric detector (Molectron J-3) and were kept at ~200 $\mu J/cm^2$ to avoid multiphoton processes. To obtain photoionization efficiency curves, the ion intensities of the mass spectra ionized by the tunable UV laser were plotted as a function of photon energy with normalization by both the laser fluence and the ion intensities of ArF ionization mass spectra. The adiabatic E_is of the $M_n(C_6H_6)_m$ clusters were determined from the final decline of the photoionization efficiency curves. The uncertainty of the E_is is estimated to be typically ±0.05 eV.

2.2. Quantum Chemical Calculations. All the calculations were performed using the GAMESS program[23] with an IBM RS6000 workstation on our local network and an IBM SP2 of the Computer Center of the Institute for Molecular Science, Japan.

One of the goals of the present paper is to reveal why vanadium atoms form multiple-decker sandwich clusters efficiently. For this purpose, we need to know the potential energy profile of not only the electronic ground state but also some lower-lying excited states having various spin or spatial symmetries.

The description of bond dissociation processes requires a method capable of accounting for the "near-degeneracy" effect at least, and we employed the full valence configurational interaction (FVCI) method. In the calculations for the M−C_6H_6 systems, we defined 10 orbitals, e_1 and e_2 of benzene and 3d and 4s of the metal atom, as valence orbitals. In addition, it is also very important to define an appropriate set of one-electron orbitals in the CI calculation. We should use a set of orbitals optimized for each state or an averaged state. In such a sense, the state-averaged MCSCF method[24] is most suitable but somewhat tedious for treating many electronic states. Then we employed the configuration-averaged SCF method[25] with a concept similar to the state-averaged MCSCF method. The configuration-averaged SCF method determines the set of orbitals that minimize the average energy of various configurations. In fact, we handled it as a special case of the open shell SCF method with a fractional occupation number and used the GVB module in the GAMESS program. Concretely, we chose the 3d and 4s orbitals as the open shell orbitals and put four, five, and six active electrons in these orbitals for Ti−, V−, and Cr−C_6H_6, respectively.

The basis set used in all the calculations was the MIDI[26] built in the GAMESS program. Here, this basis set does not have primitive functions for representing the 4p atomic orbital of the metals. To see the effect of a 4p atomic orbital, potential energy curves for the Cr−benzene system were also calculated with the TZV basis, which contains basis functions for 4p atomic orbital. The results of calculations show that the qualitative character of the states, whose asymptotic atomic states are $3d^n$, $3d^{n-1}4s^1$, and $3d^{n-2}4s^2$ configurations, was not affected by adding the 4p atomic orbital. Thus, it is considered that the MIDI basis set is enough for our qualitative discussion.

In the calculation of the potential energy profile, we changed only the distance between metal atom and the center of mass in the benzene molecule. Namely, the benzene structure was not allowed to relax and was fixed to the isolated one optimized by the CASSCF method with the $\pi(e_1)$ and $\pi^*(e_2)$ active space.

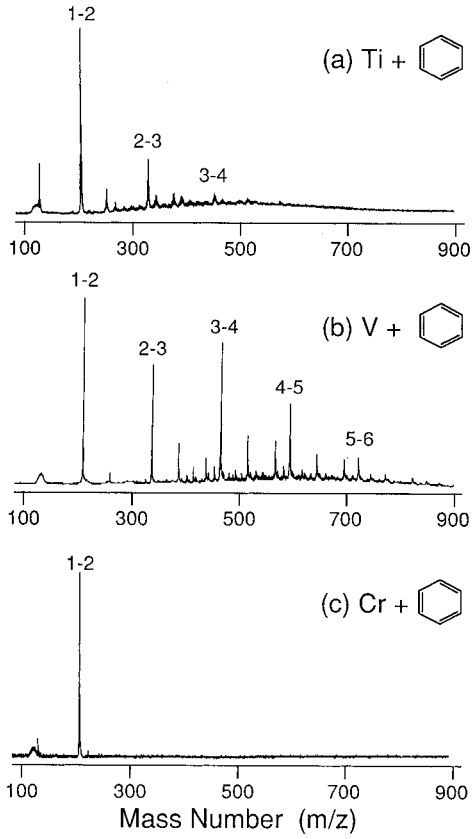

Figure 1. Time-of-flight mass spectra of $M_n(C_6H_6)_m$ clusters. Parts a, b, and c are for M = Ti, V, and Cr, respectively. Peaks of the clusters are labeled according to *n-m*, denoting the number of metal atoms (*n*) and C_6H_6 molecules (*m*). The ionization laser fluence is typically ~100 $\mu J/cm^2$.

3. Results

3.1. Mass Spectra for M−Benzene (M = Ti, V, and Cr) Systems. Figure 1 shows the mass spectra for M−benzene systems (M = Ti, V, and Cr). Peaks of the clusters are labeled according to the notations *n* and *m*, denoting the number of metal atoms (*n*) and benzene molecules (*m*). In the case of V−benzene, there is a series of major peaks in the mass number of $V_n(C_6H_6)_{n+1}$. Therefore, we have proposed the multiple-decker sandwich structure for those species and it has been proved by the experiment of the reactivity toward the CO molecule.[8] Both Ti and Cr atoms are next to the V atom on the periodic table, and it is generally regarded that these atoms resemble each other in their chemical properties. However, the patterns of the mass spectra for Ti− and Cr−benzene are not the same for V−benzene. The characteristic peak distribution implying the sandwich structure vanishes in the mass spectra for Cr−benzene and is weakened in that for Ti−benzene. We have also examined all the other first-row transition-metal−

benzene systems and have found that V atoms form the multiple-decker sandwich cluster with the benzene molecule most efficiently. The question now arises: *Why do vanadium atoms form multiple-decker sandwich clusters with benzene molecules most efficiently*? This question is the subject of the present paper.

3.2. E_i Measurements of $M(C_6H_6)_2$ (M = Ti, V, and Cr) Complexes. The *adiabatic* E_is of $M(C_6H_6)_2$ complexes were determined experimentally by the photoionization method using the tunable UV laser. Figure 2 shows the efficiency curves of the photoionization for $Ti(C_6H_6)_2$, $V(C_6H_6)_2$, and $Cr(C_6H_6)_2$. The *adiabatic* E_is obtained are 5.71(2), 5.75(3), and 5.43(1) eV for $Ti(C_6H_6)_2$, $V(C_6H_6)_2$, and $Cr(C_6H_6)_2$, respectively. These values are approximately in agreement with the *vertical* E_is previously reported[29,30] for sandwich complexes in the condensed phase by the use of photoelectron spectroscopy (see Table 1). This result suggests that the electronic states of our $M(C_6H_6)_2$ (M = Ti, V, and Cr) complexes are the same as in the condensed phase.

3.3. Potential Energy Profiles of $M-C_6H_6$ (M = Ti, V, and Cr) Systems. As will be described, we need to consider the kinetic aspects of cluster formation, and we also performed quantum chemical calculations for $M-C_6H_6$ systems (M = Ti, V, and Cr).

Before showing the results of calculations, it is useful to review their bonding scheme. In general, a 4s electron of the metal atom M has a repulsive interaction with the doubly occupied benzene a_1 orbitals (the $3d_{z^2}$ orbital also has a_1 symmetry, but its size is relatively small, and thus, the repulsive interaction is weaker than that of 4s). Thus, the ground-state metal atom having a $3d^{n-2}4s^2$ or $3d^{n-1}4s^1$ electronic configuration is repulsive toward a benzene molecule as shown in Figure 3. However, an exited state having a $3d^n$ electronic configuration with an unoccupied 4s orbital has an attractive interaction with the benzene molecule. If (i) a promotion energy from the atomic ground state to an excited state with a $3d^n$ configuration is small and (ii) a stabilization energy of this excited state from a dissociation limit to a complex region is large, these two diabatic potential energy curves should intersect each other as shown in the lower half of Figure 3. In such a case, the potential energy profile has a well and a reaction barrier derived from an avoided-crossing. On the other hand, in the case that the stabilization energy of the excited state is small, these two diabatic potential energy curves do not intersect, resulting in a ground-state adiabatic potential energy curve that is completely repulsive as shown in the upper half of Figure 3. Here, the stabilization energy is larger in the lower spin species, which can be understood readily from the orbital interaction. Namely, a high-spin species must put electrons in not only bonding or nonbonding orbitals but also antibonding orbitals. More precisely, there are two bonding (e_1, e_2), one nonbonding (a_1), and three antibonding (a_1*, e_1*, e_2*) orbitals in the valence orbitals of MC_6H_6. For example, in the case of CrC_6H_6, all the species except for the singlet must put electrons into any antibonding orbital because there are 10 valence electrons. The higher is the spin multiplicity, the more electrons are in antibonding orbitals and the smaller is the stabilization energy. Therefore, it is generally expected that the potential energy curves of the higher spin species are repulsive and those of the lower spin species have a well and a reaction barrier.

The above considerations are actually observed in the results of the FVCI calculations. Figures 4−6 show the potential energy profiles of low-lying excited states for $M-C_6H_6$, M = Ti, V, and Cr, respectively. Although more excited states were also calculated, only the lowest states within each spin multiplicity are shown in the figures for simplicity. It turns out that the potential energy curves of the septet $Cr-C_6H_6$ ($^7A_1$) and sextet $V-C_6H_6$ ($^6E_1$) are completely repulsive. This observation can be interpreted along with the "HIGH SPIN CASE" in Figure 3. The potential curves for the other states have wells and reaction barriers, which correspond to "LOW SPIN CASE" in Figure 3.

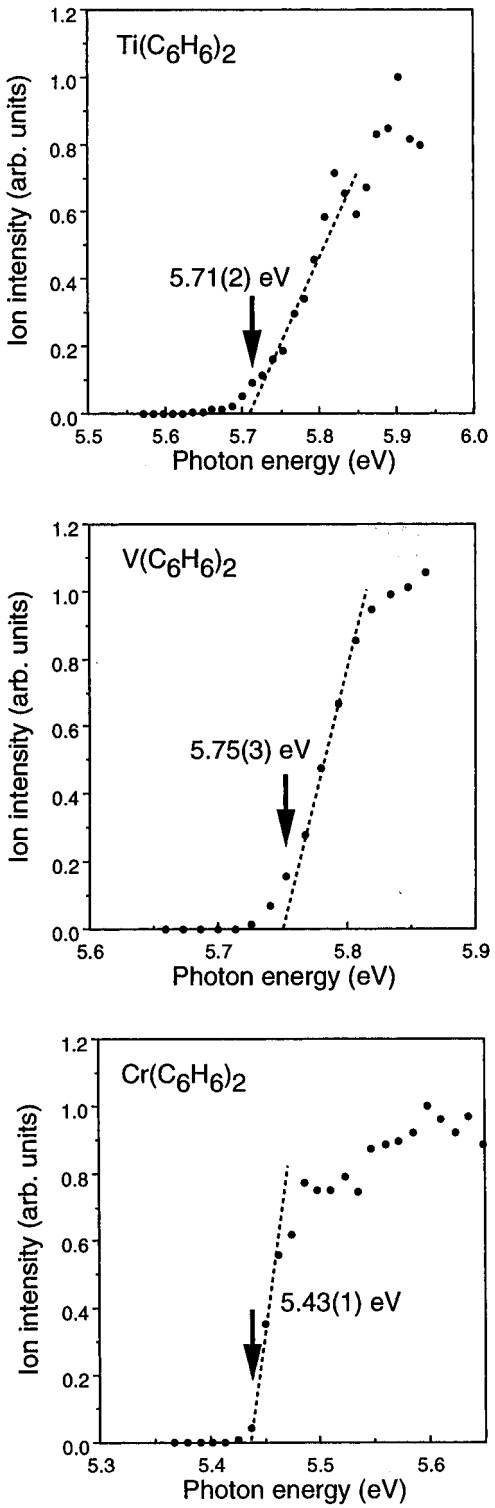

Figure 2. Photoionization efficiency (PIE) curves of $M(C_6H_6)_2$ clusters normalized by the power of the ionization laser. The photon energy was changed at ~0.015 eV intervals. From the final decline of the curve, the ionization energies of the clusters were determined to be 5.71 ± 0.02, 5.75 ± 0.03, and 5.43 ± 0.01 eV for M = Ti, V, and Cr, respectively.

TABLE 1: Ionization Energy of $M(C_6H_6)_2$ Complexes (M = Ti, V, and Cr)[c]

species	this work (adiabatic; eV)	previous work (vertical; eV)
$Ti(C_6H_6)_2$	5.71(2)	5.5−6.0[a]
$V(C_6H_6)_2$	5.75(3)	5.95[a]
$Cr(C_6H_6)_2$	5.43(1)	5.45[b]

[a] Reference 29. [b] Reference 30. [c] The differences between our adiabatic values and the vertical values obtained previously are somewhat large for M = Ti and V. This is because the first peaks in their photoelectron spectra are broad for $Ti(C_6H_6)_2$ and $V(C_6H_6)_2$. So it is expected that the electronic states of our $M(C_6H_6)_2$ (M = Ti, V, and Cr) are identical with their's in the condensed phase.

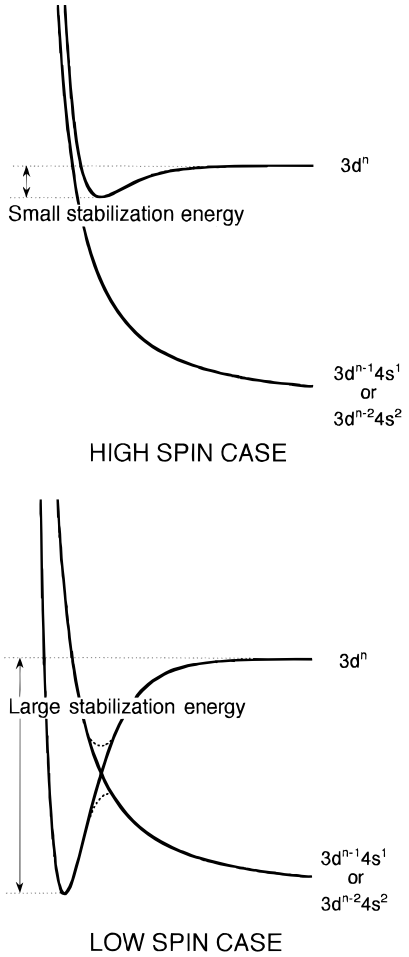

Figure 3. Schematic representation of diabatic (full lines) and adiabatic (dashes) potential energy curves for $M-C_6H_6$. The reaction coordinate is the distance between the metal atom (M) and the center of mass of the C_6H_6.

4. Discussions

4.1. Interpretation of Mass Spectra for M−Benzene (M = Ti, V, and Cr) Systems. In the interpretation of the mass spectra, both thermodynamic and kinetic stabilities should be considered. In view of the former, the species with an intense peak is considered to have thermodynamic stability. To put it more concretely, this is attributed to whether the bond between the metal atom and the ligand molecule is strong or not. Along with such an idea, several valence electron rules have been proposed. The most famous one is the 18-valence electron rule for mononuclear transition-metal complexes.

The 18-valence electron rule for the first-row transition metal complexes is derived as follows. First, valence orbitals of metal atoms are defined as 3d, 4s, and 4p orbitals. Second, the orbital interaction is composed of valence orbitals of the metal and

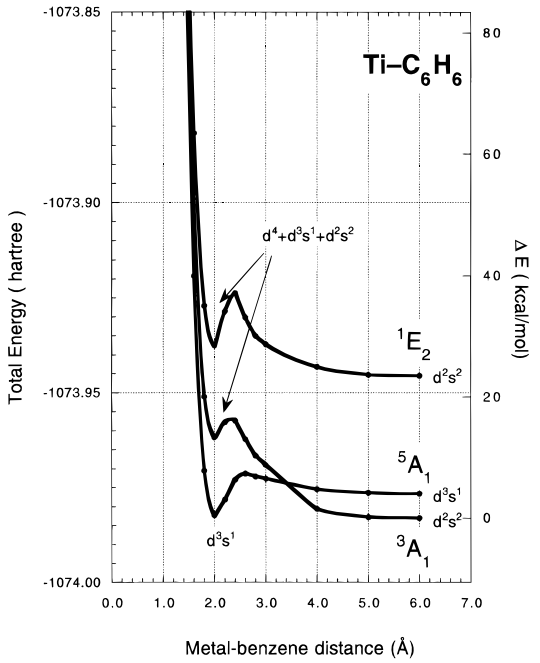

Figure 4. FVCI potential curves for the $Ti-C_6H_6$ reaction in the lowest state within each spin symmetry.

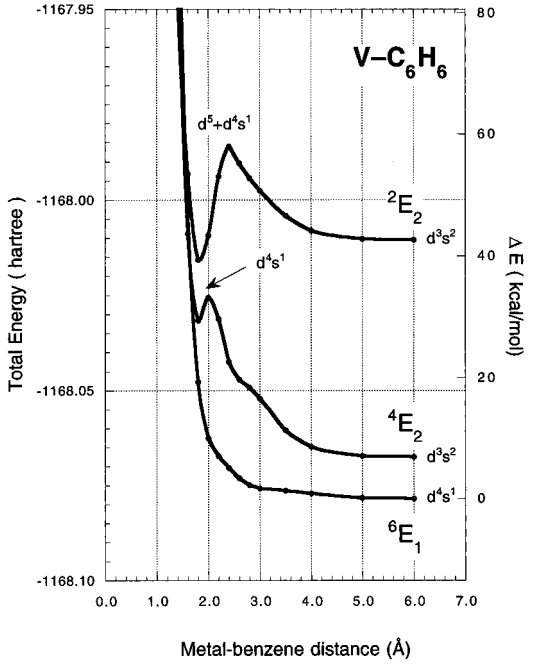

Figure 5. FVCI potential curves for the $V-C_6H_6$ reaction in the lowest state within each spin symmetry.

the ligand having the same spatial symmetries. Here, the total number of bonding orbitals and nonbonding orbitals is always 9; therefore, when the number of valence electrons is less than or equal to 18, the metal−ligand bonds are formed strongly without antibonding electrons. The numbers of valence electrons are 16, 17, and 18 for $Ti(C_6H_6)_2$, $V(C_6H_6)_2$, and $Cr(C_6H_6)_2$, respectively, and it is expected that these complexes are stable. In fact, although the preparations of these three complexes in the condensed phase have been reported, those of $M(C_6H_6)_2$ with more than 18 valence electrons have not.[10] Here, Figure 1 also shows the existence of these three complexes. All the results are therefore consistent with the 18-valence electron rule.

Lauher et al. have proposed the 30- or 34-valence electron rule for triple-decker sandwich complexes by using the fragment MO analysis.[13] Their analysis is based on the orbital interaction

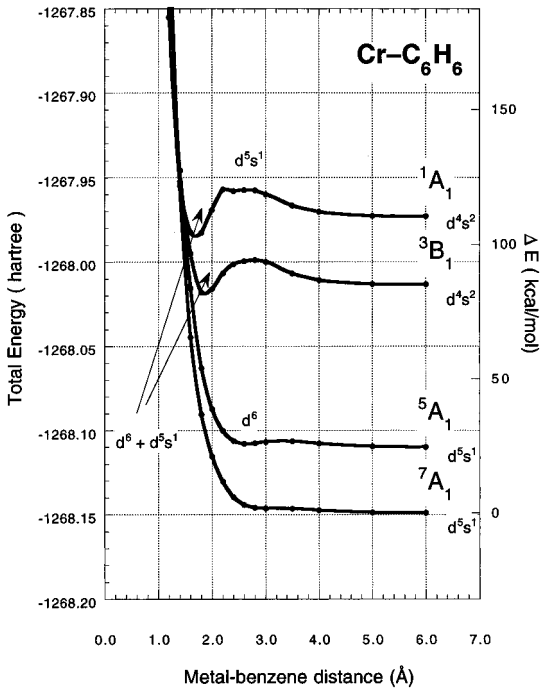

Figure 6. FVCI potential curves for the $Cr-C_6H_6$ reaction in the lowest state within each spin symmetry.

and is equivalent to the 18-valence electron rule in essence. However, the 30/34-valence electron rule cannot explain our mass spectra. The numbers of valence electrons are 26, 28, and 30 for $Ti_2(C_6H_6)_3$, $V_2(C_6H_6)_3$, and $Cr_2(C_6H_6)_3$, respectively. Although $Cr_2(C_6H_6)_3$ satisfies the valence electron rule, it is not observed at all in Figure 1. Moreover, the EHMO[27] (extended Hückel molecular orbital) electronic configurations of $M_2(C_6H_6)_3$ are

$$-(e_{2g})^4(a_{1g})^0(a_{2u})^0; \quad M = Ti$$

$$-(e_{2g})^4(a_{1g})^2(a_{2u})^0; \quad M = V$$

$$-(e_{2g})^4(a_{1g})^2(a_{2u})^2; \quad M = Cr$$

where the e_{2g} orbital is bonding with respect to the metal−benzene bond and both a_{1g} and a_{2u} orbitals are essentially localized on each metal atom and therefore nonbonding. Because the orbitals that characterize the difference of these three systems are nonbonding, one may expect the strengths of the metal−benzene bond are not so different among these three systems. However, Figure 1 shows a significant metal specificity in the formation of $M_2(C_6H_6)_3$ triple-decker sandwich clusters.

In addition to the above discussions, there is the fact that $Cr_2(C_6H_3Me_3)_3$, which has 30 valence electrons, has been synthesized and crystallized.[28] Then once $Cr_2(C_6H_6)_3$ is formed, it exists probably with thermodynamic stability. Namely, it is attributable to a kinetic factor that $Cr_2(C_6H_6)_3$ is not observed.

Judging from the above, the explanation of the metal specificity in the formation of multiple-decker sandwich clusters seems to require kinetic stability instead of thermodynamic stability, and it will be discussed in section 4.3.

4.2. Spin States of $M(C_6H_6)_2$ (M = Ti, V, and Cr) Complexes. As mentioned in section 3.2, the agreement between the E_is of $M(C_6H_6)_2$ reported previously and the ones obtained in the present work suggests that the electronic states of our $M(C_6H_6)_2$ are the same as in the condensed phase, which are sandwich complexes. The EPR experiments have clarified the spin state of $V(C_6H_6)_2$ to be a doublet,[29] and $M(C_6H_6)_2$ (M = Ti and Cr) complexes are believed to be singlets, although there are no experimental facts. Therefore, it is expected that $M(C_6H_6)_2$ in our mass spectra are singlets for M = Ti and Cr and a doublet for M = V.

It is generally expected that molecules in the condensed phase are in the ground states. To confirm the spin state of the ground state of $M(C_6H_6)_2$, theoretical calculations were also performed. The geometries of $M(C_6H_6)_2$ were optimized at the ROHF level, and the energies at these optimized geometries were calculated at the MP2 level. The results of calculations show that the ground states of $M(C_6H_6)_2$ are singlets for M = Ti and Cr and a doublet for M = V. As a result, it is concluded that the spin states of $M(C_6H_6)_2$ in our mass spectra are singlets for M = Ti and Cr and a doublet for M = V. These spin states of $M(C_6H_6)_2$ will play an important role in the discussion of the next section.

4.3. Spin Conservation and Metal Specificity in the Formation of Multiple-Decker Sandwich Clusters. As mentioned in section 4.1, the kinetic stability is needed to interpret the metal specificity in the formation of multiple-decker sandwich clusters. In other words, we must investigate the formation process itself.

There are three basic assumptions in order to explain the formation process of multiple-decker sandwich clusters. *In the first place*, it is a sequential process.[8] The sequential process means benzene molecules react not with V clusters but with V atoms sequentially. In the reaction with the V_n^+ clusters toward C_6H_6, sequential dehydrogenation channels for $V_nC_6H_k^+$ ($k < 6$) have been observed.[31] However, no dehydrogenated species were observed under our condition. Then it is concluded that the formation process of multiple-decker sandwich clusters is the sequential addition process. *In the second place*, lower spin species are more favorable. In fact, the spin multiplicity of $Cr(C_6H_6)_2$ is not a septet (Cr atom ground state) but a singlet as described in section 4.2. In a later section, this tendency will be confirmed theoretically. *In the third place*, the spin multiplicity of the system is usually conserved during the reaction because the magnitude of the spin−orbit term is relatively small for the first-row transition-metal atoms and hydrocarbon ligands. Armentrout and co-workers have proposed that the spin conservation during the reaction is a key to understanding the reaction between transition-metal atom cations and organic molecules. This idea was confirmed experimentally for many reactions.[15]

These three considerations for the formation process lead us to the simple scheme that explains the metal specificity in the formation of multiple-decker sandwich clusters. Now we concentrate on the growth process

$$M(C_6H_6)_2 + M \rightarrow M_2(C_6H_6)_2 \qquad (1)$$

In the case of M = Ti, $Ti(C_6H_6)_2$ is a singlet. The additional Ti atom is a triplet in the ground state.[32] As will be described in section 4.5, the additional atom in this process is in its ground state in general. Thus, the total spin of the reactant system is a triplet. On the other hand, the singlet species is more favorable as the product. Accordingly, the growth process (eq 1) from $Ti(C_6H_6)_2$ to $Ti_2(C_6H_6)_2$ requires a nonadiabatic transition between the two different potential energy surfaces. In the case of M = V, $V(C_6H_6)_2$ is a doublet and the additional V atom is a quartet.[32] The total spin of the reactant is a quintet or triplet. Here, our calculations showed that the triplet species of $V_2(C_6H_6)_2$ has almost the same energy as the singlet,[33] and the triplet product can be formed readily. Thus, for the V−benzene system, a transition between potential energy surfaces is not needed in reaction 1. Growth to larger multiple-decker structure,

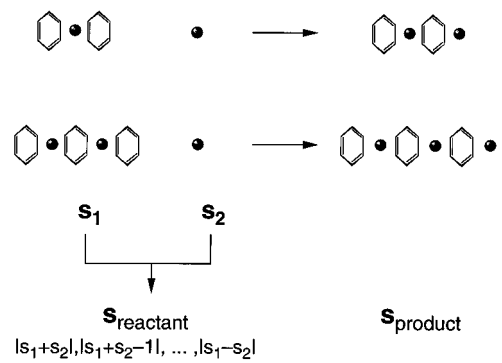

Figure 7. Proposed scheme to interpret the metal specificity observed in Figure 1. See also Table 2.

TABLE 2: Electronic Spin Multiplicity of the Reactant and the Product

	Ti	V[e]	Cr
	$M(C_6H_6)_2 + M \rightarrow M_2(C_6H_6)_2$		
s_1[a]	0	1/2	0
s_2[b]	1	3/2	3
$s_{reactant}$[c]	1	2,1	3
$s_{product}$[d]	0	1,0	0
	$M_2(C_6H_6)_3 + M \rightarrow M_3(C_6H_6)_3$		
s_1[a]	0	1	0
s_2[b]	1	3/2	3
$s_{reactant}$[c]	1	5/2,3/2,1/2	3
$s_{product}$[d]	0	3/2,1/2	0

[a] Spin of the reactant complex. [b] Spin of the reactant metal atom (ground state). [c] Spin of the overall reactant system; $s_1 + s_2$, $s_1 + s_2 - 1$, ..., $|s_1 - s_2|$. [d] Spin of the product system (lower spin species are favored to form; see text). [e] Underlined spin means that the spin is conserved in the process. Then such a process readily takes place.

therefore, takes place with no difficulty. On the other hand, $Cr(C_6H_6)_2$ is a singlet and the additional Cr atom is a septet.[32] The total spin of the reactant is a septet. The product spin is expected to be a singlet. Therefore, multiple step nonadiabatic transitions are needed for the growth from $Cr(C_6H_6)_2$ to $Cr_2(C_6H_6)_2$ in reaction 1, and it is unlikely to occur. In fact, for the Cr−benzene system, only CrC_6H_6 and $Cr(C_6H_6)_2$ have been observed.

The above discussion is summarized schematically in Figure 7 and Table 2. In Figure 7, s_1, s_2, $s_{reactant}$, and $s_{product}$ denote the spins of the reactant complex, the reactant ground-state metal atom, the overall reactant system, and the overall product system, respectively. Among them, $s_{reactant}$ is determined by the combination of s_1 and s_2, and $s_{product}$ is determined by the second assumption mentioned above that lower spin species are favorable. Table 2 shows these actual values for each case. If $s_{reactant}$ is equal to $s_{product}$, the total spin is conserved during the reaction and no spin−flip transitions between different adiabatic potential energy curves are needed in growth process 1. As seen in Figure 7 and Table 2, only the V atom is favorable for forwarding reaction 1 further to the next growth process,

$$M_2(C_6H_6)_3 + M \rightarrow M_3(C_6H_6)_3 \qquad (2)$$

This fact is also common to the following growth processes,

$$M_n(C_6H_6)_{n+1} + M \rightarrow M_{n+1}(C_6H_6)_{n+1} \qquad (3)$$

as easily generalized from Figure 7 and Table 2.

4.4. Is It True That Low Spin Species Are Favored To Form? Although the scheme proposed in the previous section can explain the metal specificity in the formation of multiple-decker sandwich clusters, it is not yet confirmed that low-spin species is favorable.

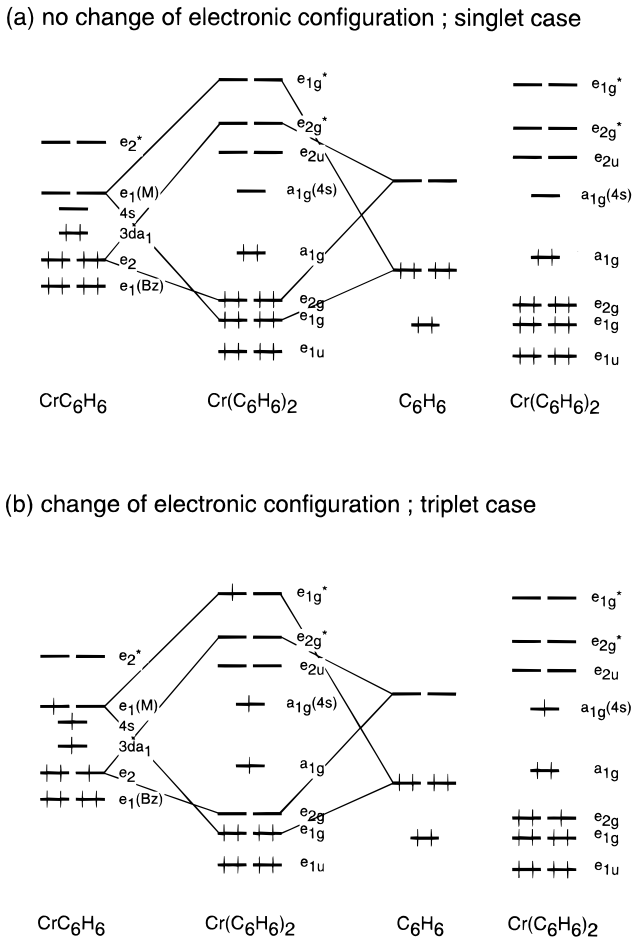

Figure 8. Electronic configuration diagrams for the benzene addition process written as $CrC_6H_6 + C_6H_6 \rightarrow Cr(C_6H_6)_2$. The electronic configuration on the right-hand side is obtained by the CISD method with RHF/ROHF orbital sets. The middle one is obtained diabatically from reactants.

As seen in section 3.3, the interaction between the transition-metal atom and benzene molecule is the donor−acceptor type, and the higher is the spin multiplicity, the more electrons are in the antibonding orbitals. So it is readily expected that lower spin species can be stable intermediates. However, the results of theoretical calculations show that intermediate spin species such as triplet Cr, quartet V, triplet Ti, and quintet Ti can also form the complex $M(C_6H_6)$. At the present stage, it cannot be concluded that lower spin species are always favored to form.

However, there is another fact to support the tendency that low-spin species are favored to form. The case of Cr is taken as a notable example in the next growth process

$$MC_6H_6 + C_6H_6 \rightarrow M(C_6H_6)_2 \qquad (4)$$

The dominant electronic configuration of the lowest triplet CrC_6H_6 at a metal−benzene distance of 1.8 Å is $(e_1;Bz)^4(3de_2)^3(3da_1)^1(4s)^1(3de_1)^1(e_2^*;Bz)^0$ as shown on the right-hand side in Figure 8b. Since the additional benzene molecule to form $Cr(C_6H_6)_2$ has occupied a_1 and e_1 orbitals, 4s and $3de_1$ electrons of CrC_6H_6 have a repulsive interaction with this additional benzene molecule. A similar discussion can be given for the lowest quintet CrC_6H_6 with the $(e_1;Bz)^4(3de_2)^2(3da_1)^1(4s)^1(3de_1)^2(e_2^*;Bz)^0$ configuration. However, the dominant electronic configuration of the lowest singlet CrC_6H_6 is $(e_1;Bz)^4(3de_2)^4(3da_1)^2(4s)^0(3de_1)^0(e_2^*;Bz)^0$. The donation from the

occupied e_1 orbital of the additional benzene to the vacant e_1 orbital of the CrC_6H_6 and the back-donation from the occupied e_2 orbital of the CrC_6H_6 to the vacant e_2 orbital of the additional benzene result in the formation of this singlet $Cr(C_6H_6)_2$. In reaction 4 for Cr, there are no repulsive interactions.

Moreover, the ground-state dominant configuration[34] of the singlet $Cr(C_6H_6)_2$ is $(e_{1g})^4(e_{2g})^4(a_{1g})^2(a_{1g})^0(e_{2u})^0(e_{2g}*)^0(e_{1g}*)^0$ and this configuration does not require a change of electronic configuration in the addition reaction process 4. Therefore, no reaction barriers exist in reaction 4 for singlet $Cr(C_6H_6)_2$. On the other hand, the ground-state dominant configuration of the triplet and quintet $Cr(C_6H_6)_2$ are $(e_{1g})^4(e_{2g})^3(a_{1g})^2(a_{1g})^1(e_{2u})^0(e_{2g}*)^0(e_{1g}*)^0$ and $(e_{1g})^4(e_{2g})^2(a_{1g})^2(a_{1g})^0(e_{2u})^1(e_{2g}*)^1(e_{1g}*)^0$, respectively. These configurations require a change of electronic configuration, and thus, there is a reaction barrier in the addition process 4. Therefore, only the singlet $Cr(C_6H_6)_2$ is selectively formed.

In the case of V, configuration state functions with an occupied $3de_1$ orbital contribute to the wave function of the quartet state more significantly than to that of doublet state. The quartet VC_6H_6 has a more repulsive interaction with the benzene molecule than the doublet one does. Moreover, although the dominant electronic configuration of the quartet VC_6H_6 at a metal−benzene distance of 1.8 Å is $(e_1;Bz)^4(3de_2)^3(3da_1)^1(4s)^1(3de_1)^1(e_2*;Bz)^0$, that of the quartet $V(C_6H_6)_2$ is $(e_{1g})^4(a_{1g})^1(e_{2g})^3(a_{1g})^1(e_{2u})^1(e_{2g}*)^0(e_{1g}*)^0$, and thus, the change of the electronic configuration is needed in addition reaction 4 for quartet $V(C_6H_6)_2$. This results in a reaction barrier in the potential energy curve. On the other hand, for the doublet species, the change of electronic configuration is not needed and the potential energy curve has no reaction barriers. Then addition reaction 4 for V prefers the doublet species to the quartet ones. This tendency is the same for the Ti case.

Judging from the above arguments, it is concluded in general that the adiabaticity in the benzene addition process 3 makes the formation of the lower spin species preferable for M = Ti, V, and Cr.

4.5. Participation of Excited-State Atoms in the Formation of MC_6H_6. Figure 6 shows that the ground-state Cr (^7S) atom does not react with benzene. This result is consistent with the evidence shown by Parnis et al., that Cr (^7S) atoms, produced by laser multiphoton dissociation (MPD) of $Cr(CO)_6$ at 559 nm, do not react with benzene molecules in the gas phase.[18] In our mass spectrum (Figure 1), however, CrC_6H_6 and $Cr(C_6H_6)_2$ are observed with high abundance, where it is expected that $Cr(C_6H_6)_2$ is a singlet from the experimental value of ionization energy, as discussed in section 3.2. These pieces of evidence suggest that excited atoms produced by laser vaporization play an important role in the reaction with benzene, which takes place immediately after the laser vaporization event. In other words, singlet $Cr(C_6H_6)_2$ is formed not by the relaxation of products derived from the ground-state Cr (^7S) atom but by the reaction of the excited singlet Cr atom, which is populated spontaneously after the laser pulse.

Mitchell and Hackett have reported that the population distribution of Fe atoms produced by MPD of $Fe(CO)_5$ at 552 nm indicates a marked non-Boltzmann distribution,[35] which means that excited atoms are produced extraordinarily. They have also shown that the relaxation of these excited atoms occurs in a few microseconds even in the fastest case. The laser vaporization technique is analogous to MPD in the sense that they are multiphoton processes, and thus, it is expected that the laser vaporization also produces excited atoms before the thermal equilibrium.

Although it has usually been considered that a carrier gas such as argon gas makes excited atoms relax to the ground state, it seems reasonable to conclude that excited atoms will survive before the reaction with benzene molecules takes place.

Here, we should notice that benzene vapor is injected in large excess under our experimental conditions. In this case, reactive singlet Cr atoms would be removed completely in the first process:

$$Cr + C_6H_6 \rightarrow CrC_6H_6 \quad (5)$$

Therefore, when the reaction proceeds to the second step,

$$Cr(C_6H_6)_2 + Cr \rightarrow Cr_2(C_6H_6)_2 \quad (6)$$

no reactive singlet atoms survive. As a result, we observed only the CrC_6H_6 and $Cr(C_6H_6)_2$ species in the mass spectrum.[36]

It therefore follows that we can synthesize multiple-decker sandwich clusters for the Cr case if we can prepare singlet Cr atoms in each step of the Cr addition reaction. In fact, under the condition that excited atoms can survive for longer times, we have found a small intensity peak of $Cr_2(C_6H_6)_3$ in the mass spectrum.[37] Moreover, we have found that the mass spectra for transition-metal atoms with high-spin ground states (Fe and Mn) are very similar to that of Cr. Namely, only MC_6H_6 and $M(C_6H_6)_2$ exist in these spectra.[37] This result also rationalizes the above discussion. Then it is reasonably concluded that the excited-state atoms play an important role in the first reaction process,

$$M + C_6H_6 \rightarrow MC_6H_6 \quad (7)$$

Of course, this discussion is also applicable to the case of M = Ti and V.

4.6. Some Aspects Observed in Theoretical Calculations. In this section, we give comments on the strange behavior in the result of theoretical calculations.

First, some potential curves in Figures 4−6 are not very smooth. In particular, the ones for the quartet $V-C_6H_6$ and singlet $Cr-C_6H_6$ have wavelike folds. This is derived from complex avoided crossings between several potential curves. This strange behavior at first glance is due to describing only the lowest states in each symmetry, and one would find smooth diabatic curves by tracing the other lower-lying states.

Second, from a methodological point of view, we notice that, as shown in Figure 5, the lowest state is calculated to be a sextet at the dissociation limit. It is well-known experimentally that the ground state of the V atom is a quartet.[32] This indicates that the FVCI calculations with the configuration-averaged SCF orbitals have a bias toward stabilizing the $3d^44s^1$ configuration more than other configurations. The MCSCF calculation with the same basis set (MIDI) and active space (metal 3d and 4s) gives that the ground state of the V atom is actually a quartet, and this error is attributed to the use of the configuration-averaged SCF orbitals. The averaged electronic configuration for V is $3d^{25/6}4s^{5/6} \approx 3d^{4.2}4s^{0.8}$, which is closer to $3d^44s^1$ than to $3d^34s^2$. The use of this set of orbitals stabilizes the sextet state (^6D; $3d^44s^1$) more than the quartet (^4F; $3d^34s^2$) and the doublet (^2G; $3d^34s^2$) states. Therefore, the excitation energy from $3d^44s^1$ to $3d^34s^2$ would be overestimated. Moreover, those between different electronic configurations show significant errors, although the energy differences between the same electronic configurations agree approximately with experimental values. In fact, although $\Delta E(^4F; 3d^34s^2 \rightarrow {}^2G; 3d^34s^2)$ in Figure 5 is ~12 000 cm^{-1} and the experimental value is 10 892 cm^{-1}, $\Delta E(^4F; 3d^34s^2 \rightarrow {}^6D; 3d^44s^1)$ in the figure is −2400 cm^{-1} and

TABLE 3: Comparison of Some Calculated and Experimental Excitation Energies of Ti, V, and Cr Atoms

	excitation energy (cm^{-1})		related state and their electronic configurations lower → upper
	exptl	calcd	
Ti	6557	1400	$^3F(3d^24s^2) \rightarrow {}^5F(3d^34s^1)$
	7255	8200	$^3F(3d^24s^2) \rightarrow {}^1D(3d^24s^2)$
V	10892	12000	$^4F(3d^34s^2) \rightarrow {}^2G(3d^34s^2)$
	2112	−2400	$^4F(3d^34s^2) \rightarrow {}^6D(3d^44s^1)$
Cr	7593	8600	$^7S(3d^54s^1) \rightarrow {}^5S(3d^54s^1)$
	8824	8900	$^3P(3d^44s^2) \rightarrow {}^1G(3d^44s^2)$
	23163	29800	$^7S(3s^54s^1) \rightarrow {}^3P(3d^44s^2)$
	31987	38700	$^7S(3d^54s^1) \rightarrow {}^1G(3d^44s^2)$

the experimental value is 2112 cm^{-1}. This tendency is generally observed in the other case (see Table 3).

If the change of an electronic configuration in the midst of potential curves exists and many electronic states are close to each other in energy, the FVCI calculation with a configuration-averaged SCF orbital set is very useful and handy for treating low-lying states globally. However, the above discussion shows that this method cannot be used for the discussion about the properties related to the relative position of potential surfaces. In the present work, we concentrate on the shapes of each potential curve.

5. Conclusion

We have found the metal specificity in the formation of multiple-decker sandwich clusters and succeeded in the explanation for this specificity with the conservation of spin and the rule that low-spin species are favored to form. The rule was actually supported by the theoretical calculations and is related to the following. (i) The interaction between metal atom and benzene molecule is the donor−acceptor type. The higher is the spin multiplicity, the more electrons are in the antibonding orbitals and the smaller is the stabilization energy. (ii) High-spin species require a change of electronic configuration in the benzene addition process, and thus, potential curves for such a process have a reaction barrier.

Our results support that the spin conservation is useful for interpreting the metal (or state) specific reaction between transition-metal atoms and organic molecules. Moreover, it is concluded that both electronic configuration and spin multiplicity are needed to understand these reactions.

Acknowledgment. We are very grateful to Dr. K. Hoshino and Mr. T. Kurikawa for valuable discussion and to Messrs. H. Takeda, M. Hirano, and K. Yagi for their experimental assistance. We also thank the Computer Center of the Institute for Molecular Science for the use of the IBM SP2 computer.

References and Notes

(1) Yeh, C. S.; Willey, K. F.; Robbins, D. L.; Pilgrim, J. S.; Duncan, M. A. *Chem. Phys. Lett.* **1992**, *196*, 233.

(2) Higashide, H.; Kaya, T.; Kobayashi, M.; Shinohara, H.; Sato H. *Chem. Phys. Lett.* **1990**, *171*, 297.

(3) Holland, P. M.; Castleman, A. W., Jr. *J. Chem. Phys.* **1982**, *76*, 4195.

(4) Robels, E. S. J.; Ellis, A. M.; Miller, T. A. *J. Phys. Chem.* **1992**, *96*, 8791.

(5) Misaizu, F.; Sanetaka, M.; Fuke, K.; Iwata, S. *J. Chem. Phys.* **1994**, *100*, 1161.

(6) Mitchell, S. A.; Blitz, M. A.; Siegbahn, P. E. M.; Svensson, M. *J. Chem. Phys.* **1994**, *100*, 423.

(7) Nakajima, A.; Taguwa, T.; Hoshino, K.; Sugioka, T.; Naganuma, T.; Ono, F.; Watanabe, K.; Nakao, K.; Konishi, Y.; Kishi, R.; Kaya, K. *Chem. Phys. Lett.* **1993**, *214*, 22.

(8) Hoshino, K.; Kurikawa, T.; Takeda, H.; Nakajima, A.; Kaya, K. *J. Phys. Chem.* **1995**, *99*, 3053.

(9) (a) Kealy, T. J.; Pauson, P. L. *Nature (London)* **1951**, *168*, 1039. (b) Miller, S. A.; Tebboth, J. A.; Tremaine, J. F. *J. Chem. Soc.* **1952**, 632.

(10) Mingos, D. M. P. In *Comprehensive Organometallic Chemistry*, 1st ed.; Wilkinson, G., Stone, F. G. A., Abel, E. W., Eds.; Pergamon Press: New York, 1982; Vol. 3, Chapter 19.

(11) (a) Werner, H.; Salzer, A. *Synth. Inorg. Met.-Org. Chem.* **1972**, *2*, 239. (b) Salzer, A.; Werner, H. *Angew. Chem.* **1972**, *84*, 949. (c) Dubler, E.; Textor, M.; Oswald, H.-R.; Salzer, A. *Angew. Chem.* **1974**, *86*, 125.

(12) Duff, A. W.; Jonas, K.; Goddard, R.; Kraus, H.-J.; Krüger, C. *J. Am. Chem. Soc.* **1983**, *105*, 5479.

(13) Lauher, J. W.; Elian, M.; Summerville, R. H.; Hoffmann, R. *J. Am. Chem. Soc.* **1976**, *98*, 3219.

(14) Kaldor, A.; Cox, D. M. *Pure Appl. Chem.* **1990**, *62*, 79.

(15) Armentrout, P. B. *Annu. Rev. Phys. Chem.* **1990**, *41*, 313. (b) Elkind, J. L.; Armentrout, P. B. *J. Phys. Chem.* **1987**, *91*, 2037.

(16) Brown, C. E.; Mitchell, S. A.; Hackett P. A. *J. Phys. Chem.* **1991**, *95*, 1062.

(17) Ritter, D.; Carroll J. J.; Weisshaar, J. C. *J. Phys. Chem.* **1992**, *96*, 10636.

(18) Parnis, J. M.; Mitchell, S. A.; Hackett, P. A. *J. Phys. Chem.* **1990**, *94*, 8152.

(19) Mitchell, S. A.; Hackett, P. A. *J. Chem. Phys.* **1990**, *93*, 7822.

(20) Bauschlicher, C. W.; Partridge, H.; Langhoff, S. R. *J. Phys. Chem.* **1992**, *96*, 3273.

(21) King, W. A.; Di Bella, S.; Lanza, G.; Khan, K.; Duncalf, D. J.; Cloke, F. G. N.; Fragala, I. L.; Marks, T. *J. Am. Chem. Soc.* **1996**, *118*, 627.

(22) Roszak, S.; Balasubramanian, K. *Chem. Phys. Lett.* **1995**, *234*, 101.

(23) Schmidt, M. W.; Baldridge, K. K.; Boatz, J. A.; Elbert, S. T.; Gordon, M. S.; Jensen, J. H.; Koseki, S.; Matsunaga, N.; Nguyen, K. A.; Su, S. J.; Windus, T. L.; Dupuis, M.; Montgomery, J. A. GAMESS. *J. Comput. Chem.* **1993**, *12*, 1347.

(24) (a) Hinze, J. *J. Chem. Phys.* **1973**, *59*, 6424. (b) Docken, K.; Hinze, J. *J. Chem. Phys.* **1972**, *47*, 4928.

(25) (a) McWeeny, R. *Methods of Molecular Quantum Mechanics*, 2nd ed.; Academic: London, 1989; Section 6-6. (b) Slater, J. C. *Quantum Theory of Atomic Structure*; McGraw-Hill: New York, 1960; Vol. II, Section 17-7.

(26) Huzinaga, S.; Andzelm, J.; Klobukowski, M.; Radzio-Andzelm, E.; Sakai, Y.; Tatewaki, H. *Gaussian Basis Sets for Molecular Calculations*; Elsevier: Amsterdam, 1984.

(27) Howell, J.; Rossi, A.; Wallace, D.; Haraki, K.; Hoffmann, R. FORTICON8. *QCPE* Program No. 517.

(28) (a) Lamanna W. M. *J. Am. Chem. Soc.* **1986**, *108*, 2096. (b) Lamanna W. M.; Gleason W. B.; Britton D. *Organometallics* **1987**, *6*, 1583.

(29) Cloke, F. G. N.; Dix, A. N.; Green, J. C.; Perutz, R. N.; Seddon, E. A. *Organometallics* **1983**, *2*, 1150.

(30) (a) Evans, S.; Green, J. C.; Jackson, S. E. *J. Chem. Soc., Fraraday 2* **1972**, *68*, 249. (b) Guest, M. F.; Hillier, I. H.; Higginson, B. R.; Lloyd, D. R. *Mol. Phys.* **1975**, *29*, 113.

(31) Zakin, M. R.; Cox, D. M.; Brickman, R. O.; Kaldor, A. *J. Phys. Chem.* **1989**, *93*, 6823.

(32) Moore, C. E. *Atomic Energy Levels*; National Bureau of Standards: Washington, DC, 1949.

(33) For the case of vanadium, the orbitals that are derived from a linear combination of the $3d^a_{z^2}$, $3d^b_{z^2}$ metal AOs localized at each vanadium atom contribute those in the HOMO−LUMO region. However, the overlap between $3d_{z^2}$ orbitals in such molecular orbitals is very small and their MOs are nonbonding. For $V_2(C_6H_6)_2$ or $V_2(C_6H_6)_3$, it is considered that the energy difference between the singlet species with the $^1(3d^a_{z^2}, 3d^b_{z^2})$ configuration and triplet species with the $^3(3d^a_{z^2}, 3d^b_{z^2})$ configuration is very small. This consideration was confirmed by the GVB−PP calculations. This result can be generalized for larger V−benzene clusters.

(34) The dominant electronic configurations of $M(C_6H_6)_2$ complexes are determined by the CISD calculation with RHF/ROHF orbital sets.

(35) Mitchell, S. A.; Hackett, P. A. *J. Chem. Phys.* **1990**, *93*, 7813.

(36) Nonreactive ^7S Cr atoms are not photoionized by the ArF laser (6.42 eV) because of their high ionization energy (6.77 eV) and do not emerge in the mass spectrum.

(37) Kurikawa, T.; Takeda, H.; Nakajima, A.; Kaya, K. Unpublished data.